

# THE WISE BLAZAR-LIKE RADIO-LOUD SOURCES: AN ALL-SKY CATALOG OF CANDIDATE $\gamma$ -RAY BLAZARS

R. D'ABRUSCO<sup>1</sup>, F. MASSARO<sup>2</sup>, A. PAGGI<sup>1</sup>, H. A. SMITH<sup>1</sup>, N. MASETTI<sup>3</sup>, M. LANDONI<sup>4</sup> & G. TOSTI<sup>5,6</sup>

version October 2, 2014: fm

## ABSTRACT

We present a catalog of radio-loud candidate  $\gamma$ -ray emitting blazars with WISE mid-infrared colors similar to the colors of confirmed  $\gamma$ -ray blazars. The catalog is assembled from WISE sources detected in all four WISE filters, with colors compatible with the three-dimensional *locus* of the WISE  $\gamma$ -ray emitting blazars, and which can be spatially cross-matched with radio sources from either one of the three radio surveys: NVSS, FIRST and/or SUMSS. Our initial WISE selection uses a slightly modified version of previously successful algorithms. We then select only the radio-loud sources using a measure of the radio-to-IR flux, the  $q_{22}$  parameter, which is analogous to the  $q_{24}$  parameter known in the literature but which instead uses the WISE band-four flux at 22  $\mu$ m. Our final catalog contains 7855 sources classified as BL Lacs, FSRQs or mixed candidate blazars; 1295 of these sources can be spatially re-associated with confirmed blazars. We describe the properties of the final catalog of WISE blazar-like radio-loud sources and consider possible contaminants. Finally, we discuss why this large catalog of candidate  $\gamma$ -ray emitting blazars represents a new and useful resource to address the problem of finding low energy counterparts to currently unidentified high-energy sources.

*Subject headings:* galaxies: active - galaxies: BL Lacertae objects - radiation mechanisms: non-thermal

## 1. INTRODUCTION

The largest known class of  $\gamma$ -ray sources is represented by the rarest class of Active Galactic Nuclei (AGNs), blazars (e.g. Abdo et al. 2010; Nolan et al. 2012). This population of radio-loud sources is mainly characterized by flat radio spectra and superluminal motions, variable and high polarization from the radio to the optical band (Urry & Padovani 1995; Massaro et al. 2009). Their emission is strongly dominated by non-thermal radiation over the entire electromagnetic spectrum, featuring two broad components in their spectral energy distributions: the low-energy one peaking between the IR and the X-ray and the high-energy one exhibiting its maximum in the  $\gamma$ -ray energies.

Blazars are historically divided in two main classes on the basis of their optical spectra. The first class includes the BL Lac objects, characterized by featureless spectra with emission/absorption lines of equivalent width lower than 5 Å (Stickel et al. 1991; Stocke et al. 1991; Laurent-Muehleisen et al. 1999). The second class is represented by the flat spectrum radio quasars (FSRQs), that show normal quasar-like spectra. In the following we adopt the nomenclature proposed in the Multi-wavelength Blazar Catalog<sup>7</sup> (BZCat, Massaro et al. 2009, 2011), that labels BL Lac objects as BZBs and FSRQs as BZQs.

The ROMA-BZCat is based on by-eye inspection of multi-frequency data and the extensive review of the literature for each member. The minimal requirements that a source has to meet to be included in the BZCat, are the optical identification and/or availability of optical spectrum, X-ray luminosity equal or larger than  $10^{43}$  erg s<sup>-1</sup> and a compact radio morphology. These stringent requirements and the use of heterogeneous data make for a very reliable but incomplete list of *bona fide* blazars. The selection of large, homogeneous samples of blazars is intrinsically difficult, because of their peculiar spectral characteristics and extreme variability. New simpler criteria can be useful to extract larger and less incomplete samples of candidate blazars, whose nature has to be confirmed through additional follow-up observations.

We have recently discovered that  $\gamma$ -ray emitting blazars have infrared colors that distinguish them from other galactic and extragalactic sources in the three-dimensional colors space of the mid-IR WISE magnitudes (Massaro et al. 2011; D'Abrusco et al. 2012). We used this result to devise a new method for the association of the *Fermi* Large Area Telescope (LAT) unidentified  $\gamma$ -ray sources through a parametrization of the region occupied by  $\gamma$ -ray blazars in the WISE colors space, the so-called WISE blazars *locus* (D'Abrusco et al. 2013; Massaro et al. 2013a).

In this paper, we present a catalog of candidate  $\gamma$ -ray emitting blazars extracted from the AllWISE Data Release<sup>8</sup>. This catalog is composed of radio-loud WISE sources detected in all four WISE filters, whose mid-IR colors are similar to the typical colors of confirmed  $\gamma$ -ray emitting blazars (see D'Abrusco et al. 2013), spatially associated to a radio source and selected as radio-loud. Hereinafter, such sources will be called “WISE Blazar-like RAdio-Loud Sources”, or WIBRaLS.

<sup>1</sup> Harvard - Smithsonian Center for Astrophysics, 60 Garden Street, Cambridge, MA 02138, USA

<sup>2</sup> Yale Center for Astronomy and Astrophysics, Physics Department, Yale University, PO Box 208120, New Haven, CT 06520-8120, USA

<sup>3</sup> INAF/IASF di Bologna, via Gobetti 101, I-40129 Bologna, Italy

<sup>4</sup> INAF/Osservatorio Astronomico di Brera, Via E. Bianchi 46, 23807 Merate, Italy

<sup>5</sup> Dipartimento di Fisica, Università degli Studi di Perugia, 06123 Perugia, Italy

<sup>6</sup> Istituto Nazionale di Fisica Nucleare, Sezione di Perugia, 06123 Perugia, Italy

<sup>7</sup> <http://www.asdc.asi.it/bzcat/>

<sup>8</sup> <http://wise2.ipac.caltech.edu/docs/release/allwise/expsup/>

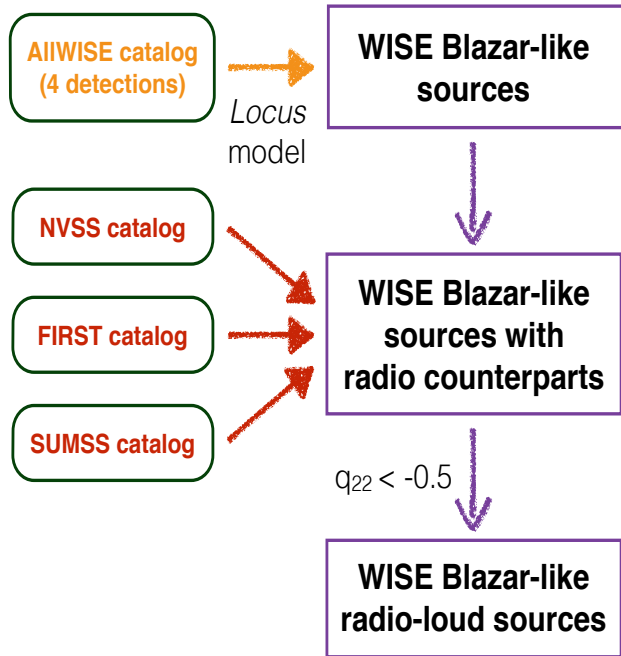


**Figure 1.** Schematic representation of the workflow for the extraction of the WIBRaLS.

The paper is organized as follows: in Section 2 we give a brief summary of the procedure used to select the WIBRaLS and the basic information about the final catalog. Specifically, in Section 2.1 we discuss the method used to select the WISE sources with IR colors similar to the colors of the  $\gamma$ -ray emitting blazars. Section 2.2 is devoted to the description of the technique used to perform the spatial association of the WISE sources with the radio counterparts, and in Section 2.3 we introduce the radio-loudness parameter  $q_{22}$  and discuss its application to select radio-loud sources among the sample of WISE blazar-like sources with a radio association. In Section 3, we describe the final catalog of WIBRaLS, and in Section 4 we compare the WIBRaLS with other WISE-based techniques optimized for the selection of AGNs (Section 4.1) and with the VERONCAT (Véron-Cetty & Véron 2010) (Section 4.2), to indirectly characterize the nature of the sources in our catalog and assess possible contamination from non-blazars. Finally, in Section 5 we summarize the results and draw our conclusions. We use cgs units and spectral indices are based on the definition of the flux density as  $S_\nu = \nu^{-\alpha}$ .

The WISE magnitudes in the [3.4], [4.6], [12], [22] $\mu$ m nominal filters are in the Vega system. The values of three WISE magnitudes, namely [3.4], [4.6] and [12], and of the colors derived using those magnitudes, have been corrected for galactic extinction according to the extinction law presented by Draine (2003).

## 2. THE SELECTION OF THE WISE BLAZAR-LIKE RADIO-LOUD SOURCES

The three steps followed to select WISE blazar-like radio-loud sources can be summarized as follows:

- WISE sources detected in all four filters [3.4], [4.6], [12], [22] $\mu$ m are selected according to their mid-IR colors, using a slightly modified version of the technique for the association of high-energy

sources with WISE candidate blazars presented by D’Abrusco et al. (2013) (see Section 2.1). We designate these sources as “WISE blazar-like sources”.

- The WISE blazar-like sources selected with the method described in Section 2.1 are positionally cross-matched with the catalogs of sources detected in three different radio surveys: NRAO VLA Sky Survey - NVSS (Condon et al. 1998)<sup>9</sup>, the Sydney University Molonglo Sky Survey - SUMSS (Mauch et al. 2003)<sup>10</sup> and the Faint Images of the Radio Sky at Twenty-cm survey - FIRST (Becker et al. 1995)<sup>11</sup>. Only the WISE blazar-like sources that can be associated to at least one radio source from either one of three radio surveys within the maximum radial distances discussed in Section 2.2 are further considered.
- We retain only the WISE blazar-like sources with radio counterpart that satisfy the radio-loudness criterion  $q_{22} \leq -0.5$  (Section 2.3), in order to minimize the contamination in our catalog from sources whose radio emission is not associated to AGN activity.

We anticipate that the final number of unique WIBRaLS selected with our method is 7855. A workflow representing the procedure for the extraction of the catalog of WIBRaLS is shown in Figure 1. In the following sections, we will discuss in details the three steps summarized above.

### 2.1. Extraction of the WISE blazar-like sources

The method for the extraction of the WISE blazar-like sources used in this paper is based on the technique for the association of the unidentified  $\gamma$ -ray sources presented by D’Abrusco et al. (2013). Here a modified version of that method will be used to extract the WISE sources with IR colors similar to the typical colors of the  $\gamma$ -ray emitting blazars from the whole sky, without any spatial constraint, while the association method in D’Abrusco et al. (2013) selected candidate blazars located in the regions of the sky where  $\gamma$ -ray source are detected.

In what follows, a brief summary of the association method will be given (see D’Abrusco et al. 2013, for a detailed description of the dataset and method). D’Abrusco et al. (2012) found that  $\gamma$ -ray emitting blazars occupy a narrow region of the three-dimensional color space associated to the four WISE filters, called the *locus*. In D’Abrusco et al. (2013), the *locus* was defined using a sample of confirmed *Fermi*  $\gamma$ -ray blazars, based on the ROMA-BZCat (Massaro et al. 2011) and the *Fermi* LAT 2FGL (Nolan et al. 2012), associated to WISE counterparts detected in all four WISE filters ([3.4], [4.6], [12], [22] $\mu$ m). The *locus* has been modeled in the three-dimensional space generated by the Principal Components (PCs) of the IR colors distribution of the WISE sources of the *locus* itself.

<sup>9</sup> <http://heasarc.gsfc.nasa.gov/W3Browse/all/nvss.html>

<sup>10</sup> <http://heasarc.gsfc.nasa.gov/W3Browse/all/sumss.html>

<sup>11</sup> <http://heasarc.gsfc.nasa.gov/W3Browse/all/first.html>

This model is composed of a set of three coaxial cylindrical regions aligned to the PC1 axis. Two cylinders are dominated by blazars of the same spectral classes, namely BZB and BZQ, while the third cylinder is positioned between these two cylinders and contains a mixed population of both BZBs and BZQs. The ranges of PC1 coordinates spanning the heights of the three cylinders were determined so that the two extreme cylinders contain at least 75% of *locus* sources classified as BZBs and BZQs, respectively. The height of the Mixed cylinder was set accordingly. The radii of the three cylinders are determined so that 90% of the sources whose PC1 coordinate lies within the PC1 ranges of each cylinder, lie within the respective cylinder (see Figure 3 and Table 2 of D’Abrusco et al. 2013).

The position of a generic WISE source relative to each of the three distinct cylinders in the model of the *locus*, is used to choose the sources most likely to have the typical WISE colors of the  $\gamma$ -ray emitting blazars. We called the quantitative measure of the compatibility of the position of a generic WISE source with each of the three cylinders of the model, separately, the *score*. The score can be calculated in two steps: 1) the WISE colors of the source (and corresponding uncertainties) are projected into the PC space, where an error ellipsoid is defined; 2) the position of the ellipsoid relative to the *locus* model is translated to a numeric value, the *score*, which varies continuously between zero and one, and is weighted by the volume of the error ellipsoid in the PC space (see Section 3.2 of D’Abrusco et al. 2013, for the definition of *score*). In general, the larger the *score values*, the closer the source to the *locus* model and the more similar the WISE colors to the colors of the confirmed  $\gamma$ -ray emitting blazars.

In D’Abrusco et al. (2013) the sources with null scores were discarded, while WISE sources with non-null *scores* were classified in three classes, namely A, B and C, based on *score* thresholds defined as the 90%-th, 60%-th and 20%-th percentiles of the *score* distribution of the *locus* sample, separately for each of the three regions of the *locus*. The three classes A, B and C are sorted according to decreasing compatibility with the model of the *locus*: class A sources are considered to be the most likely WISE blazar-like sources, while the positions of class B and class C sources are still compatible with the model of the *locus* but at a lesser degree than class A sources.

In this paper, we use the same approach described in D’Abrusco et al. (2013) to determine the value of the *score* thresholds, except for the percentile associated to the lowest threshold. In order to select the largest possible number of WISE blazar-like sources, we set the three thresholds to the 20%-th, 60%-th and 90%-th percentiles of the *score* distribution of the *locus* sample (see Figure 2 and compare with Figure 6 in D’Abrusco et al. 2013). The adoption of a lower threshold for the definition of the class C sources makes our selection more complete but, at the same time, potentially increases the contamination of the class C from sources that only marginally have WISE colors similar to the colors of the confirmed WISE  $\gamma$ -ray emitting blazars. The presence of class C contaminants is mitigated by considering only the WISE blazar-like sources which can be positionally associated with sources in either one of the three radio surveys (NVSS, FIRST,

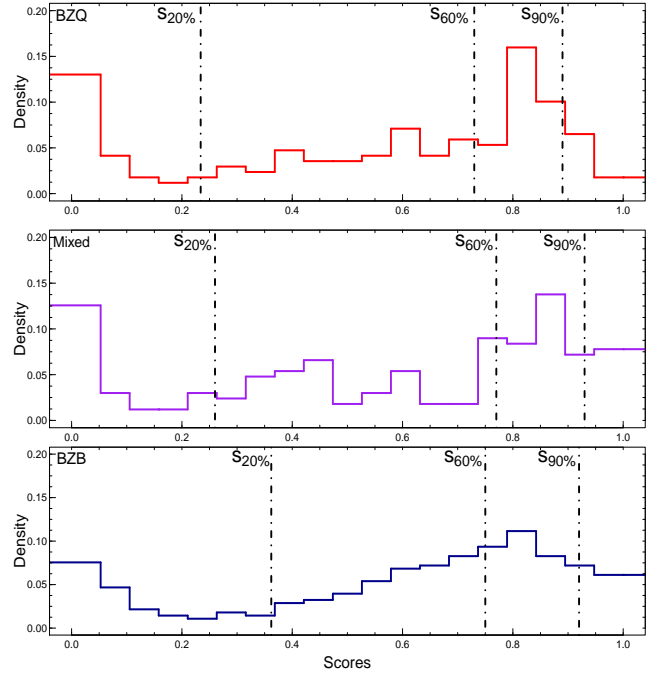


**Figure 2.** Histograms of distributions of *score* values for the sources in the sample used to define the *locus* model (see Section 2.1) for the three regions of the *locus* model occupied by BZQs, the BZBs and in the mixed region (upper, lower and mid panels respectively). The three dashed vertical lines in each panel represent the values of the *score* associated with the 20%-th, 60%-th and 90%-th percentiles for BZBs, BZQs and mixed sources respectively.

SUMSS) used in this paper (Section 2.2).

For each distinct region of the model (BZB, BZQ or Mixed), class A sources have score  $s \geq s_{90\%}$ , class B sources have score  $s_{60\%} \leq s < s_{90\%}$  and class C sources have score  $s_{20\%} \leq s < s_{60\%}$ . The values of the *score* thresholds derived from the score distributions of the sources in the *locus* for the three regions of the model are reported in Table 1. Each source with score larger than the  $s_{20\%}$  threshold for one of the cylinders of the model, is assigned the corresponding type (BZB, BZQ or Mixed). The WISE blazar-like sources whose type are BZB or BZQ have IR colors similar to the colors of the *bona fide* WISE-detected  $\gamma$ -ray emitting blazars classified as BZB or BZQ, respectively. The type Mixed, conversely, does not indicate any particular spectral class since the Mixed cylinder contains comparable fractions of both BZBs and BZQs.

The total number of WISE blazar-like sources selected by our method is 265170 (see Table 3), split in 32789 BZB-type candidates, 169703 BZQ-type candidates and 62678 sources compatible with the Mixed region of the *locus*. The sample of 265170 WISE blazar-like sources is split in 3554 ranked as Class A, 17500 as Class B and the remaining 244116 classified as Class C candidates. The Class C candidates represent  $\sim 92\%$  of the total number of WISE blazar-like sources, while the Class A and Class B candidates account only for the  $\sim 1.3\%$  and  $\sim 6.6\%$ , respectively. These fractions result from the conservative choices of the *score* thresholds used to define the classes of the sources based on their WISE colors and uncertainties (see D’Abrusco et al. 2013 for more details).

## 2.2. Spatial crossmatch with radio catalogs

**Table 1**

Values of the *score* thresholds  $s_{20\%}$ ,  $s_{60\%}$  and  $s_{90\%}$ , used for the extraction of the WISE blazar-like sources. These values are determined as the 20%-th, 60%-th and 90%-th percentiles of the distribution of *scores* of the *locus* sample split by BZB, Mixed and BZB regions.

	BZB	Mixed	BZQ
$s_{20\%}$	0.36	0.26	0.23
$s_{60\%}$	0.75	0.77	0.79
$s_{90\%}$	0.92	0.93	0.89

In order to determine the optimal radius for the spatial association of the WISE blazar-like sources with the radio sources in the NVSS, the SUMSS and FIRST catalogs, we used a modified version of the procedure used by Donoso et al. (2009) and Best et al. (2005). In these two papers, the authors determined the optimal radius for the spatial association of NVSS and FIRST radio sources to optical sources in SDSS by setting a threshold on the fraction of spurious associations (i.e. the contamination) obtained for different values of the maximum association radius.

In this paper, we will use as optimal association radius the radial distance corresponding to a given fixed efficiency of the selection  $e_{\text{thr}} = 99\%$ <sup>12</sup>, corresponding to a contamination  $c_{\text{thr}} = 1\%$  where the contamination is defined as  $c(r) = 100\% - e(r)$ . This choice of the efficiency has the result of minimizing the fraction of spurious sources selected and optimize the success likelihood of the follow-up observations required to confirm their nature, at the cost of a limited completeness. The efficiency of the selection is defined as the number of sources around real radio positions  $n^{\text{real}}(r)$  minus the number of sources around the mock radio positions  $n^{\text{mock}}(r)$ , expressed as a fraction of the number of real cross-matches. For a given radius  $r$ , the efficiency  $e(r)$  is defined as:

$$e(r) = 100 * \left( \frac{n^{\text{real}}(r) - n^{\text{mock}}(r)}{n^{\text{real}}(r)} \right) \quad (1)$$

We have estimated  $n^{\text{real}}(r)$  by counting the number of WISE sources detected in all four bands within circular regions of radius  $r$  between  $0''$  and  $60''$  centered on a sample of  $5 \cdot 10^4$  sources randomly extracted from each of the three radio surveys. In order to estimate the corresponding  $n^{\text{mock}}(r)$  values, we have created one hundred mock realizations of the coordinates of each real radio source by shifting its position by a radial distance randomly drawn from the interval  $[60, 120]''$  in a random direction. The numbers of WISE sources associated to real and mock radio positions are shown in the upper panels of Figure 3 as functions of the radial distance (real and mock crossmatches are shown as solid and dashed black curves respectively). The numbers of crossmatches around mock positions can be fractional as they have been averaged over the 100 mock realizations of the real radio positions. The lower panels in Figure 3 show the contamination  $c(r)$ , calculated with the equation 1, as a function of the radial distance from the radio coordinates. In the lower panels the horizontal line correspond-

ing to the threshold contamination  $c_{\text{thr}} = 1\%$  (efficiency  $e(r) = 99\%$ ) and the vertical lines indicate the optimal radii, corresponding to the intersection of the horizontal lines with the completeness curve.

The optimal cross-match radii determined with this method are  $r_{\text{NVSS}} = 10.3''$ ,  $r_{\text{SUMSS}} = 7.4''$  for the NVSS and SUMSS surveys, respectively. The number of WIRaLS sources with distinct NVSS and SUMSS radio counterparts selected, as a consequence, is 11928 and 2325, respectively.

Our method does not produce a reasonable estimate of the optimal radius for the FIRST survey (see right plot in Figure 3), likely because of the very high density of FIRST sources in the sky compared to the other two surveys. The black solid line in the right plot of Figure 3 declines very steeply at small radial distances, with  $\sim 85\%$  of the total crossmatches found at distances smaller than  $5''$ . Based on this fact, we have adopted a different approach to determine a crossmatch radius for FIRST. We have chosen as optimal radial distance three times the combined positional uncertainties of AllWISE and FIRST detections. The maximum allowed positional uncertainty of AllWISE detections along each axis is  $0.5''$ <sup>13</sup>, even though for most of the sources detected the error is  $\sim 0.02''$  per axis, yielding a total positional uncertainty of  $\sim 0.1''$ . In order to be conservative in our analysis, we have assumed a positional uncertainty for AllWISE sources  $\sigma_{\text{W1}} = 0.5''$ . The astrometric accuracy of FIRST radio sources down to the survey flux threshold is consistently better than  $1''$  (White et al. 1997). Nonetheless, also in this case we will assume a conservative positional uncertainty  $\sigma_{\text{FIRST}} = 1''$  for FIRST detections. Thus, the combined positional uncertainty can be estimated as  $\sigma_{\text{W1+FIRST}} = \sqrt{\sigma_{\text{W1}}^2 + \sigma_{\text{FIRST}}^2} \sim 1.12''$ , which yields an optimal radius for FIRST sources  $r_{\text{FIRST}} = 3\sigma_{\text{W1+FIRST}} = 3.4''$ . Using this maximum radial distance, we select 106 WIRaLS sources with FIRST radio counterparts that cannot be associated to a NVSS source.

We do not attempt to estimate the completeness of our selection procedure because the properties of the parent population of our sample of WIRaLS are impossible to determine. In the case of the FIRST survey, the adoption of a smaller maximum radial distance compared to the radii used for NVSS and SUMSS surveys, possibly results in a lower completeness. However, we estimate the loss of real crossmatches to be small: the increase in the number of sources selected with our procedure using radial distance  $r = 10''$  is only 104, corresponding to  $\sim 10\%$  of the number of WIRaLS selected with the optimal radius  $r_{\text{FIRST}} = 3.4''$ .

The number of WISE blazar-like sources with at least one radio counterpart within the maximum radial distances discussed above is 11928, 6592 and 2325 for NVSS, FIRST and SUMSS surveys, respectively (see Table 3), for a total of 20845 WISE blazar-like sources spatially associated to distinct radio counterparts from either of these three catalogs. We find that 1552 WISE blazar-like sources are associated to one NVSS and one SUMSS radio source, while 3660 WISE blazar-like sources are cross-matched to one NVSS and one FIRST radio sources. For

<sup>12</sup> In this paper, we call “efficiency” the same quantity called “reliability” by Best et al. (2005)

<sup>13</sup> See [http://wise2.ipac.caltech.edu/docs/release/allwise/expsup/sec2\\_5.html](http://wise2.ipac.caltech.edu/docs/release/allwise/expsup/sec2_5.html) for details

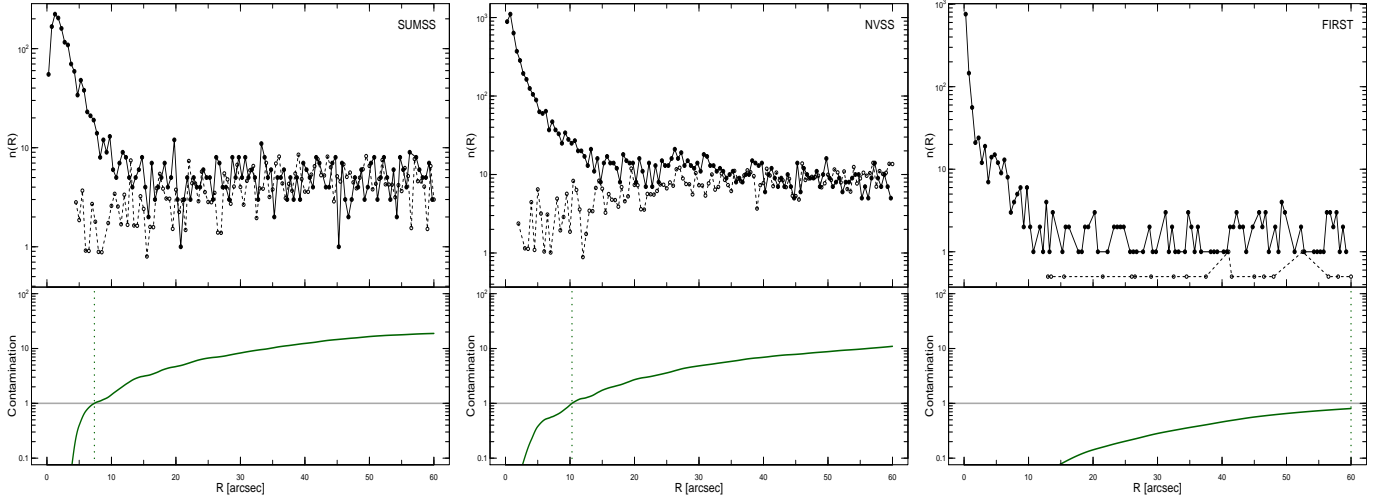


**Figure 3.** Upper panels: number of real cross-matches (solid lines) and mock cross-matches (dotted lines) for WISE sources detected in all bands as function of the radial distance  $r$  in the interval  $[0'', 60'']$ , for SUMSS, NVSS and FIRST surveys (from left to right). Lower panels: contamination of the selection procedure for radial distances in the interval  $[0'', 60'']$  for each of the three radio surveys used in this paper. The horizontal lines show the contamination threshold  $c_{\text{thr}} = 1\%$  and the vertical lines indicate the optimal radii for NVSS and SUMSS surveys, chosen as described in Section 2.2. For FIRST survey, the procedure used to select the optimal crossmatch radius employed in this paper is different (see Section 2.2).

this reason, the final number of unique WISE blazar-like sources with at least one radio counterpart is 16632.

### 2.3. Radio-loudness Selection

Blazars are by definition radio-loud AGNs. For this reason, in our analysis we only consider WISE blazar-like sources that can be spatially associated to at least one radio counterpart in one of the three radio surveys within the maximum radial distance discussed in Section 2.2. However, radio emission can be also produced by physical mechanisms not due to the presence of an AGN. For example, it is well known that the far-IR and radio emission are tightly and linearly correlated in star-forming systems (see e.g., Sargent et al. 2010; Bonzini et al. 2012, and references therein for more details). The strength of the correlation between radio and far-IR emissions is usually expressed via the so-called  $q$  parameter, defined as the logarithm of the ratio of far-IR to radio flux density, (e.g., Helou et al. 1985). Unfortunately, flux density measurements at far-IR frequencies required to compute the  $q$  parameter are often not available. However, Padovani et al. (2011) and Bonzini et al. (2013) have recently shown that it is possible to define a  $q_{24}$  parameter as:

$$q_{24} = \log(S_{24\mu\text{m}}/S_{1.4\text{GHz}}) \quad (2)$$

where  $S_{24\mu\text{m}}$  is the observed flux density at  $24\mu\text{m}$  and  $S_{1.4\text{GHz}}$  is the flux density measured at 1.4 GHz. The use of the observed flux densities minimizes the uncertainties introduced by the modeling of the spectral energy distribution (Bonzini et al. 2013). It is worth noting that the  $24\mu\text{m}$  band of the Multi-band Imaging Photometer for *Spitzer* (MIPS), used to measure the  $S_{24\mu\text{m}}$  in the previous analyses, is similar to the WISE  $[22]\mu\text{m}$  band<sup>14</sup> (Wright et al. 2010; Cutri et al. 2011). The passbands of the WISE  $[22]$  and MIPS-24 band are similar, al-

though the  $[22]$  WISE filter is slightly bluer in response<sup>15</sup>. For all the WISE blazar-like sources associated to one radio source using the method described in Section 2.2, we calculated the  $q_{22}$  parameter as follows:

$$q_{22} = \log(S_{22\mu\text{m}}/S_{\text{radio}}) \quad (3)$$

Following Bonzini et al. (2013), we used the flux density at 1.4 GHz as the radio flux density  $S_{\text{radio}}$ . Since flux density measurements at 1.4 GHz are not available in the SUMSS survey, for the SUMSS counterparts we used the flux densities at 843 MHz instead. A well known property of the blazars is the flatness of their radio spectra (see e.g., Healey et al. 2007) that extends up to low radio frequencies well below 1 GHz (see also Massaro et al. 2013a,c,d, 2014, for a recent discussion). For this reason, the use of the flux density at 843 MHz instead of the flux density at 1.4 GHz to estimate the  $q_{22}$  parameter affects negligibly our analysis. Nonetheless, we checked that the differences introduced in the value of the parameter  $q_{22}$  by the use of the flux density measured at 843 MHz instead of the flux density at 1.4 GHz are small. We used the 553 WISE blazar-like sources with one radio counterpart in the SUMSS catalog and another in the NVSS catalog (see Section 2.2). For these sources we calculated  $q_{22}$  parameter values using both flux densities measured at 1.4 GHz and 843 MHz. Figure 4 shows the  $q_{22}(1.4\text{ GHz})$  vs  $q_{22}(843\text{ MHz})$  distribution for this sample of sources. The difference between the values of  $q_{22}(1.4\text{ GHz})$  and  $q_{22}(843\text{ MHz})$  for all the WISE blazar-like sources with radio counterparts in the two surveys is smaller than 10% of the  $q_{22}(1.4\text{ GHz})$  value for  $\sim 88\%$  of the sources. We also notice that the distribution of the differences between the values of the two values of  $q_{22}$  peaks at  $\Delta q_{22} = q_{22}(843\text{ MHz}) - q_{22}(1.4\text{ GHz}) \sim 0.08$  and does not depend on the WISE spectral class of the sources considered. Moreover,  $\Delta q_{22}$  is almost constant over the range of  $q_{22}$  spanned by our sample of WISE blazar-like sources with

<sup>14</sup> [http://wise2.ipac.caltech.edu/docs/release/allsky/expsup/sec6\\_3a.html](http://wise2.ipac.caltech.edu/docs/release/allsky/expsup/sec6_3a.html) <sup>15</sup> [http://wise2.ipac.caltech.edu/docs/release/prelim/expsup/sec4\\_3g.html](http://wise2.ipac.caltech.edu/docs/release/prelim/expsup/sec4_3g.html)



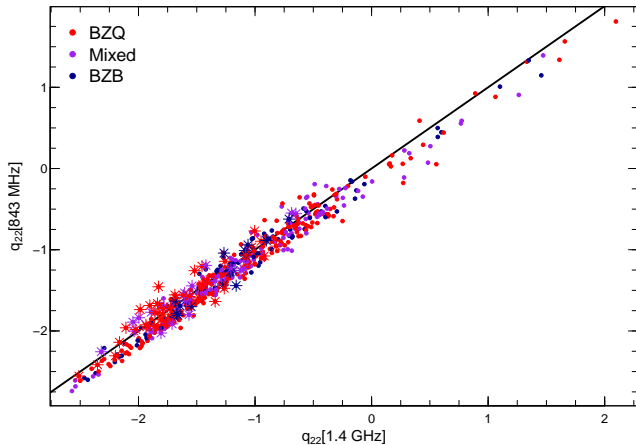


**Figure 4.** Values of the  $q_{22}[1.4 \text{ GHz}]$  and  $q_{22}[843 \text{ MHz}]$  parameters for all WISE blazar-like sources associated to a radio counterpart in both the NVSS and SUMSS surveys. The stars represent the 73 confirmed blazars in this sample that can be cross-matched to a BZCat counterpart. The spectral classification of the WISE blazar-like sources based on their WISE colors (see Section 2.1) is color-coded.

radio counterparts in both the NVSS and SUMSS surveys. For this reason, for radio-loud WISE blazar-like radio sources with only SUMSS radio counterpart, we have used the corrected  $q'_{22}(843 \text{ MHz}) = q_{22}(843 \text{ MHz}) + \Delta q_{22}$  where  $\Delta q_{22} = 0.08$ . The change in the number of sources selected using the corrected  $q'_{22}$  is anyway  $\sim 3.5\%$  of the total sample of WIBRaLS (see Section 3). It is worthwhile to stress that the scatter of the two  $q_{22}$  estimates for the subset of 73 candidate blazars in this sample associated to a confirmed blazar of the ROMA-BZCat catalog within  $3.3''$  (stars in Figure 4) is smaller ( $\sigma_{\Delta q_{22}} = 0.12$ ) and their distribution is less biased ( $\langle \Delta q_{22} \rangle = 0.01$ ) than the distribution of the whole sample. Nonetheless, we have used the correction  $\delta q_{22} = 0.08$  derived from the whole sample because the nature of most WISE blazar-like sources with radio counterparts has not been confirmed yet.

Bonzini et al. (2013) showed that the  $q_{24}$  parameter has a redshift dependence (see Figure 2 in Bonzini et al. 2013): the  $q_{24}$  values of all classes of sources considered (radio-loud AGNs, radio-quiet AGNs and star-forming galaxies) become smaller for larger redshifts. For this reason, the boundary between the regions of the redshift vs  $q_{24}$  plane (Figure 2 in Bonzini et al. 2013) dominated by the radio-loud AGNs and the other radio sources is also function of the redshift. In principle, if redshift estimates for all WISE blazar-like sources associated to a radio counterpart were available, we could have removed the redshift dependence and selected radio-loud WISE blazar-like sources with a radio counterpart at each redshift. Since redshifts are not available, we can only set a fixed threshold for the  $q_{22}$ <sup>16</sup>. Figure 5 shows the distribution of  $q_{22}$  values calculated for the confirmed  $\gamma$ -ray emitting blazars in the *locus* sample as a function of the

redshifts and color-coded according to their spectral classification from the BZCat. We have excluded the sources of the *locus* (mostly BZBs) whose redshifts are not well determined or unknown. All *locus* sources have  $q_{22}$  lower than 0 and  $\sim 96.5\%$  have  $q_{22} \leq -0.5$  ( $\sim 94\%$  for sources classified as BZB - blue points - and  $\sim 99\%$  for sources classified as BZQ - red points). Based on these observational evidences, we will require WIBRaLS sources to have  $q_{22} \leq -0.5$  in order to minimize the contamination from radio-quiet AGNs which can have similar WISE colors, at the cost of decreasing the overall completeness of the selection by less than 5%.<sup>17</sup>

It is interesting to discuss how  $q_{22} \leq -0.5$  condition affects the completeness of our selection. By assuming completeness limits of  $\sim 2.5 \text{ mJy}$  at 1.4 GHz for NVSS catalog (Condon et al. 1998),  $\sim 1 \text{ mJy}$  at 1.4 GHz for FIRST (Becker et al. 1995) and  $\sim 8 \text{ mJy}$  at 843 MHz (Mauch et al. 2003), and with a flux limit  $\sim 6 \text{ mJy}$  in the WISE [22] filter (coverage depth 11,  $\text{SNR} = 11$ )<sup>18</sup>, the nominal value for our selection  $q_{22} \leq -0.5$  (see Figure 5) at the WISE  $22\mu\text{m}$  limit therefore implies a flux density in the radio  $\geq 20 \text{ mJy}$ , within the detection limit of all the radio catalogs. Therefore our WISE-selected sample should be complete in this regard. On the other hand, some fainter blazars detected in the radio may have escaped detection with WISE in the [22] filter, and the BZB class would be most likely to suffer from this deficit because, typically, the synchrotron peak of their spectral energy distributions is at higher energies than FSRQs. Future deep mid-IR followups, perhaps with the James Webb Space Telescope, might extend the sample of *bona fide* blazars with measured mid-IR properties.

We have explored the possibility that Steep-Spectrum Radio Quasars (SSRQs) contaminate the sample of WIBRaLS selected with our method. The SSRQs are powerful radio sources characterized by radio spectral index  $\alpha_R > 0.5$ , usually calculated between 1.4 GHz and 4.85 GHz. In order to evaluate the contamination from SSRQs, we have used a sample of 18 *bona fide* SSRQs selected by Gu & Li (2013) among the SDSS optical quasars in the Stripe 82 region and with radio counterparts in the FIRST, PMN and GB6 surveys. The cross-match of the SSRQs radio positions with the WISE All-WISE catalog within a maximum radius  $3.4''$  (the cross-match radius for FIRST radio counterparts estimated in Section 2.2) yields 18 unique WISE counterparts. Two of these WISE counterparts not detected in the W4 band have been discarded. The application of the WISE colors selection method described in Section 2.1 to the 16 remaining WISE SSRQs counterparts produced 11 sources selected as WISE blazar-like sources, all classified as BZB-type candidates. The distribution of the  $q_{22}$  values for the WISE counterparts of the 11 SSRQs spans the interval  $[-2.2, 0.3]$ , and 8 of them ( $\sim 73\%$ ) have  $q_{22} \leq -0.5$ ,

<sup>16</sup> The determination of the redshifts of BZBs can be intrinsically difficult, because of the lack of significant features in their optical spectra. In order to increase the number of confirmed blazars with reliable spectroscopy, we are carrying out an extensive observational program to acquire the spectra of a large number of WISE-selected candidate blazars. The first results are discussed in Paggi et al. (2014)

<sup>17</sup> We have also evaluated the effect of the redshift distribution on the distribution of the  $q_{22}$  values of the WISE blazar-like sources and on the fraction of sources selected by the  $q_{22} \leq -0.5$  condition. We have calculated the  $q_{22}$  values for each confirmed  $\gamma$ -ray emitting blazars in the *locus* sample after varying its redshift on a regularly spaced grid in the interval  $[0, 4]$ , and assuming a power-law spectral energy distribution with slope defined by the observed flux densities at  $22\mu\text{m}$  and at 1.4GHz. We found that  $\sim 94\%$  of the estimated  $q_{22}$  values for all redshift values are still smaller than -0.5.

<sup>18</sup> [http://wise2.ipac.caltech.edu/docs/release/allwise/expsup/sec2\\_3a.html](http://wise2.ipac.caltech.edu/docs/release/allwise/expsup/sec2_3a.html)

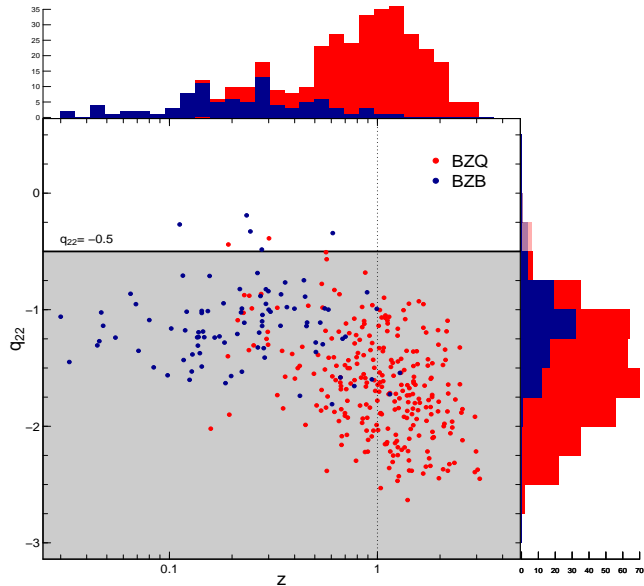


**Figure 5.** Scatterplot of the  $q_{22}$  values for the confirmed  $\gamma$ -ray emitting blazars in the *locus* sample as a function of their redshifts (from the BZCat), with marginal histograms (*locus* sources with undetermined or uncertain redshifts are excluded). The black solid line shows the threshold  $q_{22} \leq -0.5$  used to select the WIBRaLS (see discussion in Section 2.3).

i.e. are compatible with the  $q_{22} \leq -0.5$  condition used to extract the WIBRaLS. Therefore, 50% of the SSRQs sample produced by Gu & Li (2013) is included in the WIBRaLS catalog. We found that the WIBRaLS catalog can contain SSRQs and that it is not possible to selectively exclude this class of sources using the  $q_{22}$ , since their  $q_{22}$  values have similar distribution to the  $q_{22}$  values for the confirmed  $\gamma$ -ray emitting blazars. While a quantitative estimate of the contamination from SSRQs contaminants based on this small sample is impossible, we discuss this point further in Section 4.2.

The distribution of the  $q_{22}$  values for all sources in the catalog of WISE blazar-like sources with at least one radio counterpart, color-coded according to the WISE spectral classification in BZB-type, BZQ-type candidates and sources compatible with the Mixed region of the *locus* model, is shown in Figure 6. The solid colors represent the sources selected as WIBRaLS based on the criterion  $q_{22} < -0.5$ . The distribution of  $q_{22}$  values for the sources classified as BZB-type candidates and Mixed show only one peak located in the  $-1.5 < q_{22} < -0.5$  range, while the distribution of  $q_{22}$  values for sources classified as BZQ is clearly bimodal, with another peak at  $q_{22} \sim 0.5$ .

The number of total distinct WISE blazar-like sources with a radio counterpart selected as WIBRaLS is 10002. Using the  $q_{22} \leq -0.5$  criterion, we selected 6362, 1775 and 1865 distinct radio sources in the NVSS, FIRST and SUMSS surveys respectively (see Table 3). The final number of unique WIBRaLS is 7855 (see Table 3). In Section 3, we provide more details on the composition of the final catalog of WIBRaLS.

### 3. THE WIBRaLS CATALOG

We applied the three-steps procedure described in Section 2 to the whole WISE AllWISE Catalog of sources detected in all four WISE filters, selecting a total of  $\sim 2.65 \cdot 10^5$  WISE blazar-like sources (the composition

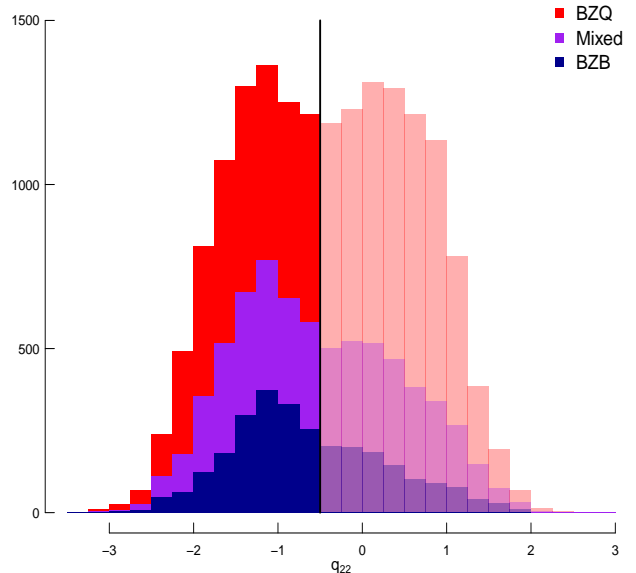


**Figure 6.** Histogram of the distribution of the  $q_{22}$  values for all the WISE blazar-like sources associated to a radio counterpart in one of the surveys used in this paper (BZB-type candidates are blue, BZQ candidates red and sources associated to the Mixed region are magenta). The full colors show the histogram of the final catalog of WIBRaLS, obtained with  $q_{22} \leq -0.5$ .

of this sample in terms of WISE classes and types is shown in Table 3). Then, we selected the WISE blazar-like sources that can be spatially associated to one radio source from three radio surveys, namely the NVSS, SUMSS and FIRST surveys, using the optimal radii established in Section 2.2. We found a total of 20845 WISE blazar-like sources with at least one counterpart from either one of the three radio surveys. In particular, 11928, 6592 and 2325 WISE blazar-like sources have a unique radio counterpart in the NVSS, FIRST and SUMSS surveys, respectively. 3660 WISE blazar-like sources can be associated to one source in both the NVSS and FIRST surveys and 553 WISE blazar-like sources can be associated to one radio source in both the NVSS and SUMSS surveys, respectively. For consistency, in the case of multiple radio counterparts from distinct surveys, we have always adopted as final radio counterpart of the WISE blazar-like source the NVSS source (FIRST and SUMSS footprints do not overlap), because NVSS covers the largest area among the radio surveys used in this paper. The final list of single distinct radio counterparts of our sample of WISE blazar-like sources contains 11928 NVSS sources, 2932 FIRST sources and 1772 SUMSS sources (see Table 3), for a total of 16632 WISE blazar-like sources with a unique radio counterpart. We finally extract the catalog of WIBRaLS by selecting only the WISE blazar-like sources with a radio counterpart with radio-loudness parameter  $q_{22} \leq -0.5$  (see Section 2.3 for details on the  $q_{22}$  parameter and the selection performed).

The final catalog of WIBRaLS contains 7855 unique sources that satisfy all our criteria: 6362 of these WISE sources are associated to a NVSS counterpart, 1407 to a source in the SUMSS survey and the remaining 86 can be cross-matched to a unique source from the FIRST survey (Table 3). The final WIBRaLS sample, according

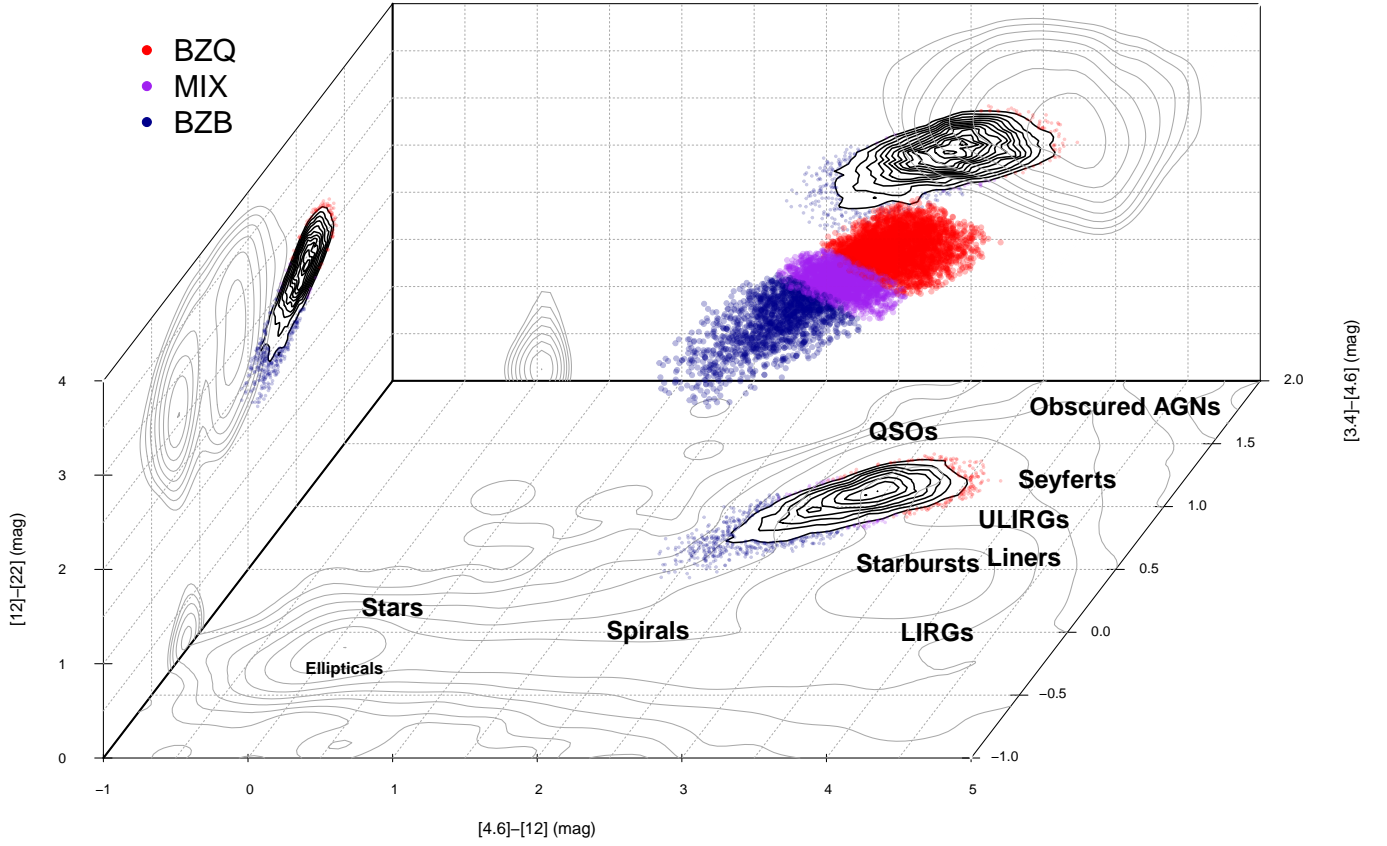


**Figure 7.** Three dimensional distribution of the sources in the WIBRaLS catalog (each source is color-coded according to the WISE spectral classification) in the space generated by the WISE [3.4]–[4.6], [4.6]–[12] and [12]–[22] colors. The black and gray lines displayed on the three planes represent the projected isodensity contours associated to ten log-spaced levels of the three-dimensional distribution of WIBRaLS and of a sample of random sources detected in all four WISE filters, respectively. The approximate locations of different typical classes of objects in the [4.6]–[12] vs [3.4]–[4.6] color-color plane, according to Wright et al. (2010), are also shown.

to the spectral classification based on the WISE colors and discussed in Section 2.1, is composed of 1682 sources classified as BZB, 3973 sources classified as BZQ and 2194 sources whose colors are compatible with the Mixed region of the *locus* model. The WIBRaLS can also be split in 129 class A sources ( $\sim 2.4\%$  of the total sample, 714 class B sources ( $\sim 9.1\%$ ) and 7012 class C sources ( $\sim 89\%$ ). These fractions are similar to the class fractions for the sample of WISE blazar-like sources before the selection based on the radio counterparts and  $q_{22}$  radio-loudness parameters (Section 2.1). They follow from the stringent definition of Class A (see Section 2.1) in terms of the threshold on the WISE *score*. The composition of the final WIBRaLS catalog is shown in Table 3.

Among the 7855 WIBRaLS, 1295 sources ( $\sim 16.5\%$ ) can be spatially re-associated to a known blazar listed in the ROMA-BZCAT (v4.1)<sup>19</sup> (Massaro et al. 2009, 2011) within  $3''.3$  (see also D’Abrusco et al. 2012, 2013, for the choice of this association radius), corresponding to  $\sim 41\%$  of the 3149 total members of the ROMA-BZCat. Moreover, 454 of the 1295 ROMA-BZCat counterparts of the

WIBRaLS can be spatially associated to a  $\gamma$ -ray emitting source of the *locus* sample ( $\sim 76.5\%$ ), extracted from the 2FGL catalog (Nolan et al. 2012) of  $\gamma$ -ray sources. This fraction is lower than the 81% fraction of *locus* sources contained, by definition, in the model of the *locus* in the WISE colors space (D’Abrusco et al. 2013). The fraction of confirmed ROMA-BZCat sources in the *locus* sample that can be spatially associated to one member of the WIBRaLS catalog ( $\sim 76.5\%$ ) is also significantly lower than the 96.5% of *locus* sources selected by directly applying the condition on the  $q_{22}$  value to their radio and WISE counterparts (see Section 2.3). The reason for the discrepancy between the 81% of the *locus* sample contained in the *locus* model by definition, and the  $\sim 76.5\%$  of *locus* sources that are selected as WIBRaLS can be found in the significant differences between the WISE photometry of  $\sim 10\%$  of the *WISE counterparts of the locus* sources in the AllSky release used to define the *locus* model by D’Abrusco et al. (2013) and the photometry in the AllWISE WISE release, used here.

The distribution of the final catalog of WIBRaLS in the three dimensional space generated by the WISE colors [3.4]–[4.6], [4.6]–[12] and [12]–[22], is shown in

<sup>19</sup> <http://www.asdc.asi.it/bzcat/>



Figure 7, where each source is color-coded according to the spectral class assigned based on its WISE colors. The three projections of the WIBRaLS 3D WISE colors distribution onto the three color-color planes clearly show that, in each plane, the peaks of the density distributions lie in the regions occupied by the sources classified as BZQ. Moreover, in Figure 7,  $10^5$  generic WISE sources located at high galactic latitude ( $|b| \geq 15^\circ$ ) and detected in all four filters have been used to plot the gray arbitrary log-spaced isodensity contours. The comparison with the black density contours of the WIBRaLS dataset shows that significant overlap between the distributions of WIBRaLS and generic WISE sources in each of the three color-color diagrams can only be removed in the 3D WISE colors space.

The sky distribution in galactic coordinates of all WIBRaLS, color-coded according to their WISE spectral class, is shown in Figure 8. The sky density of this sample depends on the spatial density of the sources in the WISE photometric catalog, whence the WISE sources with colors compatible with the *locus* of the  $\gamma$ -ray emitting blazars are extracted, and from the surface density of the three radio surveys. Contrary to the radio surveys that reach an almost homogenous depth over their footprints, the limiting sensitivity of the WISE catalog in each band is not uniform on the sky (cp. with Figure 8 at the Explanatory Supplement to the AllWISE Data Release Products<sup>20</sup>). An excerpt of the catalog of WIBRaLS is shown in Table 4. The catalog contains the following columns: WIBRaLS unique name, AllWISE WISE name, Right Ascension and Declination of the WISE source position, values of the three WISE colors and their uncertainties (corrected for galactic absorption), values of the scores for the BZB, BZQ and Mixed regions of the *locus* model, WISE-based type and spectral class, name of the final radio counterpart associated to the WISE source and value of the  $q_{22}$  parameter. The whole catalog will be available through VizieR and as a Cone Search service through all tools compatible with the Virtual Observatory (VO) specifications.

#### 4. DISCUSSION

The nature of candidate blazars can only be confirmed through optical spectroscopic follow-up observations or by collecting extensive multi-wavelength photometric data to model their spectral energy distribution. Several recent efforts have validated the nature of a large number of candidate blazars, selected with different techniques and associated to unidentified  $\gamma$ -ray sources in the 2FGL, using new and archival spectroscopic data (Shaw et al. 2013; Masetti et al. 2013; Paggi et al. 2014; Landoni et al. 2014; Massaro et al. 2014b). Nonetheless, given the current lack of observations that would firmly establish the nature of the whole sample of WIBRaLS, the only valuable information about the nature of the catalog discussed in this paper can be indirectly inferred by comparison of our sample with similarly WISE-based AGN selection techniques (Section 4.1). The comparison with the AGN selection techniques allows us to rule out significant contamination from non-AGNs, especially in the more numerous subclass of WIBRaLS classified as BZQ. This comparison also underlines the significant dif-

ference in the WISE colors of the WIBRaLS classified as BZB (BL Lacs) compared to the FSRQs subclass and the general population of radio-quiet mid-IR AGNs. Finally, in order to identify the possible contamination in our WIBRaLS catalog from AGNs not classified as blazars, in Section 4.2 we also discuss the intersection of our sample and one of the largest compilation of AGNs, QSOs and BL Lacs available, the VERONCAT (Véron-Cetty & Véron 2010).

##### 4.1. Comparison with Other WISE-based AGNs Selection Techniques

Selection techniques for AGNs based on their photometric mid-IR properties have become commonplace with the availability of WISE data. Most such techniques have been fine-tuned to identify AGNs usually selected by other mid-IR colors (*Spitzer*) and their X-ray emission. In this Section, we will compare the sample of WIBRaLS with WISE-based selection criteria from Jarrett et al. (2011); Stern et al. (2012); Mateos et al. (2012); Assef et al. (2013). In the following, the essential description of each of these selection techniques will be given.

- (A) Jarrett et al. (2011) defined a region of the  $[4.6] - [12]$  vs  $[3.4] - [4.6]$  WISE color-color diagram (the WISE AGNs “box”), using the *Spitzer* colors classification criteria determined by Stern et al. (2005) to validate the WISE selection. The AGNs box is defined as the region of the  $[4.6] - [12]$  vs  $[3.4] - [4.6]$  diagram bounded by the constant lines:  $[4.6] - [12] > 2.2$ ,  $[4.6] - [12] < 4.2$  and  $[3.4] - [4.6] < 1.7$  and the relation  $[3.4] - [4.6] > 0.1([4.6] - [12]) + 0.38$ .
- (B) Stern et al. (2012) defined a WISE color criterion  $[3.4] - [4.6] \geq 0.8$  for sources with magnitude  $[4.6] < 15.0$ , which identifies  $\sim 62 \pm 5.4$  AGNs per  $\text{deg}^2$ . This condition selects 78% of the *Spitzer* AGN candidates selected as discussed in Stern et al. (2005), with an efficiency of 95%.
- (C) Assef et al. (2013) extended the selection proposed by Stern et al. (2012) based on the WISE photometry in the  $[3.4]$  and  $[4.6]$  bands to provide a parametrized criterion that can be changed to maximize either the efficiency or the completeness of the selection. The general form of the constraint is  $[3.4] - [4.6] > \alpha_R \exp[\beta_R([4.6] - \gamma_R)^2]$ . In this paper, we have used two different sets of the parameters  $[\alpha_R, \beta_R, \gamma_R]$ , namely  $[\alpha_R, \beta_R, \gamma_R] = [0.662, 0.232, 13.97]$  and  $[\alpha_R, \beta_R, \gamma_R] = [0.530, 0.183, 13.76]$ , which yield efficiencies 90% and 75%, respectively (Assef et al. 2013).
- (D) Mateos et al. (2012) presented a selection based on the WISE magnitudes in the  $[3.4]$ ,  $[4.6]$  and  $[12]$  bands, defined in a wedge bounded by the following constraints:  $[4.6] - [12] \geq 2.517$  and  $0.315([4.6] - [12]) - 0.222 < [3.4] - [4.6] < 0.315([4.6] - [12]) + 0.796$ . This method takes into account uncertainties on the WISE photometry of the sources and is able to recover  $\sim 97\%$  and  $\sim 77\%$  of the type-1 and type-2 bona-fide AGNs observed in the Bright Ultra-Hard XMM-Newton Survey (Mateos et al. 2013). The

<sup>20</sup> [http://wise2.ipac.caltech.edu/docs/release/allwise/expsup/sec4\\_2.html](http://wise2.ipac.caltech.edu/docs/release/allwise/expsup/sec4_2.html)

**Table 2**

Total number of sources in the catalog of WISE blazar-like sources (left table), the catalog of WISE blazar-like with radio counterparts (mid), and the catalog of WIBRaLS ( $q_{22} \leq -0.5$ , right table), split for WISE class and type (see Section 2.1). Where applicable, the numbers of radio counterparts for each radio survey are also shown. The right side table shows the spectral classes and WISE-based partition in classes for WIBRaLS sources (multiple radio counterparts of WISE blazar-like sources are counted separately).

WISE blazar-like sources					WISE blazar-like sources with radio counterparts				WIBRaLS			
	BZB	Mixed	BZQ	Total	BZB	Mixed	BZQ	Total	BZB	Mixed	BZQ	Total
Class A	1345	519	1690	3554	193	236	783	1212	45	30	86	161
Class B	3985	3611	9904	17500	536	635	1663	2834	244	220	476	940
Class C	27459	58548	158109	244116	2694	4583	9522	16799	1813	2507	4581	8901
Total	32789	62678	169703	265170								
					NVSS	2093	3217	6618	1352	1804	3206	6362
					FIRST	864	1615	4113	349	468	958	1775
					SUMSS	466	622	1237	401	485	979	1865
					Total	3423	5454	11968	2012	2757	5143	10002

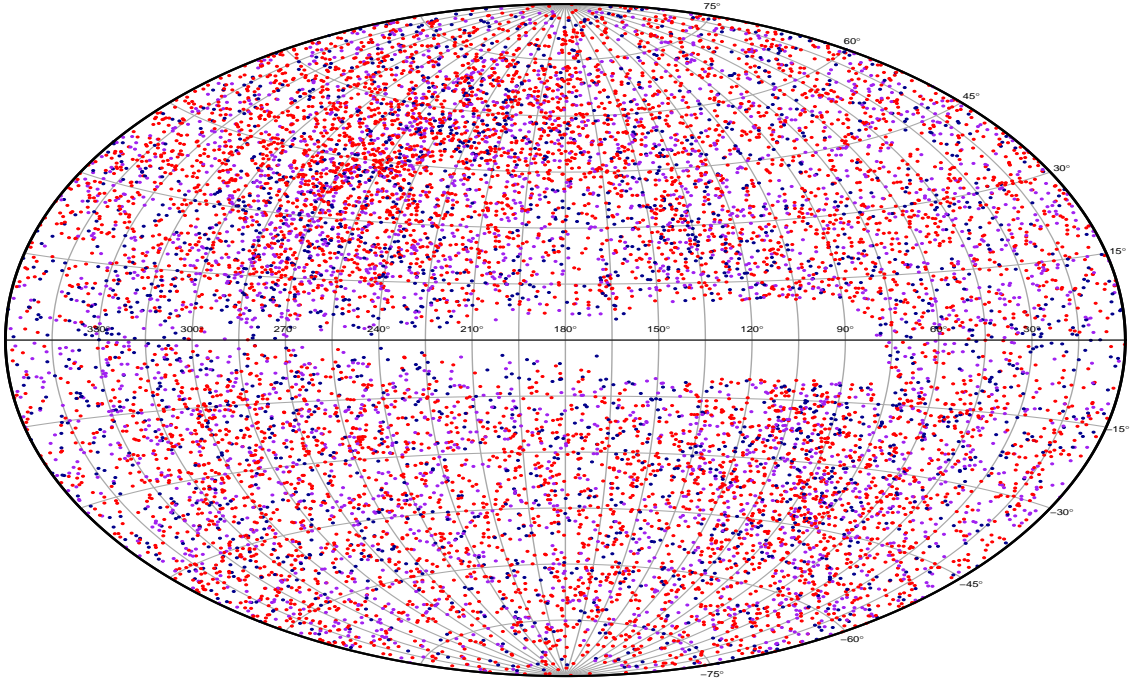


**Figure 8.** Aitoff projection of the sky distribution in galactic coordinates of the catalog of WIBRaLS, color-coded according to their WISE spectral classification in BZB, BZQ or Mixed. The empty region is not covered by any of the three radio surveys used in this paper to associate the WISE blazar-like sources.

same authors discuss a modified WISE-based AGN selection techniques that employs photometry in all four WISE filters. We will not consider this further selection technique in this paper because it attains smaller efficiency and completeness (Mateos et al. 2012).

The projections of the WIBRaLS distribution onto the WISE  $[4.6] - [12]$  vs  $[3.4] - [4.6]$  color-color plane and the  $[3.4] - [4.6]$  vs  $[4.6]$  color-magnitude plane are shown in Figure 9. The regions of the two planes used to select

the AGNs according to the four AGN selection methods described above are overplotted to the distribution of the WISE blazar-like radio sources.

We have applied the four distinct AGNs selection criteria to the 7855 members of the catalog of WIBRaLS. The numbers and fractions of WIBRaLS selected as candidate AGNs by each of the four AGN selection methods, split according to their spectral classification based on their WISE colors, are reported in Table 5 and shown in Figure 10.

**Table 3**

Composition of the final WIBRaLS catalog (only the final radio counterparts from the three radio surveys shown), in terms of WISE spectral types, classes and provenance of the radio counterpart (the NVSS sources have always been considered as radio counterparts whenever available).

	BZB	Mixed	BZQ	Total
Class A	37	26	66	129
Class B	187	165	362	714
Class C	1458	2003	3551	7012
NVSS	1352	1804	3206	6362
FIRST	21	21	44	86
SUMSS	309	369	729	1407
Total	1682	219	3973	7855

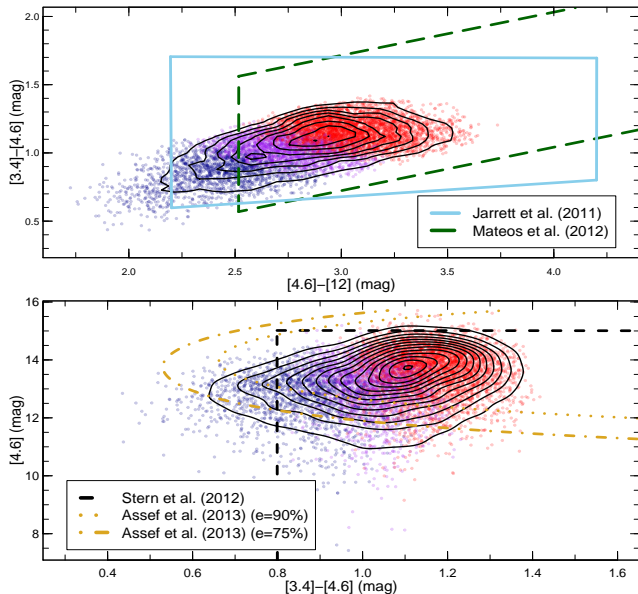


**Figure 9.** Upper panel: projection of the distribution of WIBRaLS onto the  $[4.6]-[12]$  vs  $[3.4]-[4.6]$  WISE color-color plane. The regions used by the AGN selection techniques from Jarrett et al. (2011) and Mateos et al. (2012) are also shown. Lower panel: projection of the distribution of WISE blazar-like radio sources onto the  $[3.4]-[4.6]$  vs  $[4.6]-[12]$  WISE color-magnitude plane, showing also the curves used to select AGNs according to (Stern et al. 2012) and Assef et al. (2013) (the yellow dotted line represent the selection with  $e=90\%$ , the dashed-dotted line the selection with  $e=75\%$ ). In both panels, the WIBRaLS are color-coded according to their WISE-based spectral classification, with red, blue and magenta symbols associated to sources classified as BZQ, BZB and Mixed, respectively. Moreover, the two-dimensional density distributions of the whole WIBRaLS catalog in the two planes are represented by the isodensity contours (black solid lines).

The selection methods from Jarrett et al. (2011) and Stern et al. (2012) recover the largest fractions of WIBRaLS sources (97% and 94% respectively). The criterion from Assef et al. (2013) with efficiency  $e=75\%$ , selects 90% of the whole sample of WIBRaLS, while the same method with selection efficiency  $e=90\%$  and the method from Mateos et al. (2012), both recover 75% and 85% of our catalog, respectively. Figure 10 shows the percentage of WIBRaLS selected as AGN candidates by each methods for each WISE spectral class. The fractions of WIBRaLS classified as BZQ and in the Mixed region that are selected as AGNs by either of the four methods discussed is larger than 90%, while the corre-

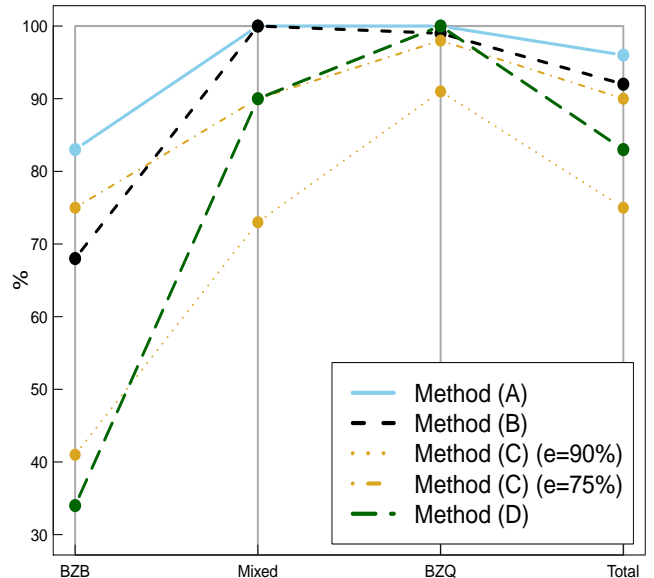


**Figure 10.** Fractions of WIBRaLS, split according to the spectral class and for the whole sample, selected as AGNs by the five methods discussed in Section 4.1.

sponding fractions of WIBRaLS classified as BZB are significantly lower, spanning from  $\sim 35\%$  of the Mateos et al. (2012) method to the  $\sim 84\%$  of the Jarrett et al. (2011) method.

The total fraction of WIBRaLS sources not selected by either one of these AGN selection techniques is  $\sim 5\%$ , almost entirely ( $\sim 94\%$ ) classified as BZB by our method (Figure 9). The total fraction of WIBRaLS classified as BZB selected by any of the five AGN selection techniques used is  $\sim 68\%$ . On the other hand, the fact that WIBRaLS classified as BZQ are overwhelmingly selected as AGNs by each of the methods considered (see Table 5) is explained by the large overlap between the region occupied by the WIBRaLS classified as candidate BZQ and the AGNs box in the two-dimensional WISE  $[3.4]-[4.6]$  vs  $[4.6]-[12]$  color space (see upper panel in Figure 9 and discussion in Wright et al. 2010; Jarrett et al. 2011; D’Abrusco et al. 2012). The BZQ-type WIBRaLS have mid-IR properties which are similar to the mid-IR and optical properties of generic quasars and, more specifically, to the population of radio-quiet AGNs usually selected by mid-IR based techniques. The contamination from non-FSRQs in the WIBRaLS catalog is further reduced by selecting only sources that can be positionally associated to radio counterparts and with  $q_{22}$  values compatible with the values of confirmed blazars. A relevant fraction of the WIBRaLS classified as BZB (from  $\sim 15\%$  to  $\sim 65\%$  for the AGN selection methods in Table 5) are bluer than the typical AGNs in WISE and, for this reason, are not selected by the techniques discussed in this Section.

#### 4.2. Cross-match with the VERONCAT

We have positionally cross-matched the WIBRaLS catalog with the Veron Catalog of Quasars & AGN (VERONCAT) (Véron-Cetty & Véron 2010) (v13). The VERONCAT is an inhomogeneous compilation of known AGNs, containing  $\sim 1.7 \times 10^5$  sources in its 13th version. Sources in the VERONCAT are broadly classified

Table 4

Sample of rows of the catalog of WIBRaLS. The complete catalog in electronic format will be available on Vizier and as a Cone Search service through all VO-compatible tools.

WIBRaLS <sup>a</sup> name	WISE <sup>b</sup> name	R.A. <sup>c</sup> deg	Dec. <sup>d</sup> deg	$c_{12}$ <sup>e</sup> mag	$\sigma_{c_{12}}$ <sup>f</sup> mag	$c_{23}$ <sup>g</sup> mag	$\sigma_{c_{23}}$ <sup>h</sup> mag	$c_{34}$ <sup>i</sup> mag	$\sigma_{c_{34}}$ <sup>j</sup> mag	$s_{BZB}$ <sup>m</sup>	$s_{MIX}$ <sup>n</sup>	$s_{BZQ}$ <sup>o</sup>	Type <sup>p</sup>	Class <sup>q</sup>	Radio <sup>r</sup> name	$q_{22}$ <sup>s</sup>
WB J0004-4736	J000435.65-473619.6	1.149	-47.605	1.09	0.03	3.32	0.03	2.31	0.07	0.0	0.0	0.83	BZQ	B	SUMSSJ000435-473620	-1.65
WB J0005+1609	J000559.23+160949.0	1.497	16.164	1.06	0.03	2.61	0.03	2.36	0.06	0.0	0.87	0.0	MIXED	B	NVSSJ000559+160946	-1.48
WB J0005+3820	J000557.18+382015.1	1.488	38.338	1.1	0.03	3.27	0.03	2.68	0.03	0.0	0.0	0.95	BZQ	A	NVSSJ000557+382015	-0.87
WB J0005+5428	J000504.36+542825.0	1.268	54.474	1.09	0.04	2.47	0.06	2.37	0.13	0.0	0.7	0.0	MIXED	C	NVSSJ000504+542825	-1.43
WB J0005-1648	J000517.92-164804.4	1.325	-16.801	1.02	0.04	2.46	0.06	2.41	0.18	0.11	0.54	0.0	MIXED	C	NVSSJ000517-164805	-1.61
WB J0005-2758	J000558.54-275857.7	1.494	-27.983	1.01	0.03	2.4	0.06	2.23	0.22	0.53	0.11	0.0	BZB	C	NVSSJ000558-275900	-1.79
WB J0005-4518	J000536.67-451845.6	1.403	-45.313	1.11	0.05	2.69	0.12	2.64	0.33	0.0	0.08	0.32	BZQ	C	SUMSSJ000537-451848	-0.66
WB J0005-6223	J000527.13-622302.6	1.363	-62.384	1.21	0.04	2.87	0.05	2.58	0.13	0.0	0.0	0.71	BZQ	C	SUMSSJ000527-622302	-0.73
WB J0006+1235	J000623.05+123553.1	1.596	12.598	1.29	0.03	2.81	0.03	2.32	0.07	0.0	0.0	0.41	BZQ	C	NVSSJ000623+123553	-1.03
WB J0006+3422	J000607.37+342220.4	1.531	34.372	1.06	0.04	2.66	0.06	2.03	0.21	0.32	0.21	0.0	BZB	D	NVSSJ000607+342220	-1.01

- Notes:  
<sup>a</sup> WIBRaLS name (IAU format)  
<sup>b</sup> WISE name  
<sup>c</sup> Right Ascension  
<sup>d</sup> Declination  
<sup>e</sup> [3.4]–[4.6] WISE color (corrected for galactic extinction)  
<sup>f</sup> Uncertainty on the [3.4]–[4.6] WISE color  
<sup>g</sup> [4.6]–[12] WISE color (corrected for galactic extinction)  
<sup>h</sup> Uncertainty on the [4.6]–[12] WISE color  
<sup>i</sup> [12]–[22] WISE color (corrected for galactic extinction)  
<sup>j</sup> Uncertainty on the [12]–[22] WISE color  
<sup>m</sup> Score for the BZB region of the *locus*  
<sup>n</sup> Score for the Mixed region of the *locus*  
<sup>o</sup> Score for the BZQ region of the *locus*  
<sup>p</sup> Spectral type (see Section 2.1)  
<sup>q</sup> Class (see Section 2.1)  
<sup>r</sup> Name of the radio counterpart  
<sup>s</sup>  $q_{22}$  value

Table 5

Fraction of WIBRaLS selected as AGNs by three distinct WISE-based selection methods: method (A) (Jarrett et al. 2011), method (B) (Stern et al. 2012), method (C) (Assef et al. 2013) and method (D) (Mateos et al. 2012). The selection technique discussed in (Assef et al. 2013) is applied with two different sets of parameters associated to efficiencies  $e=90\%$  and  $e=75\%$  respectively. In parenthesis, the fraction of selected sources relative to the number of WIBRaLS in each spectral class.

	WISE			
	BZB	Mixed	BZQ	Total
Method (A)	1396 ( $\sim 83\%$ )	2194 (100%)	3979 (100%)	7569 ( $\sim 96\%$ )
Method (B)	1136 ( $\sim 68\%$ )	2192 ( $\sim 100\%$ )	3928 ( $\sim 99\%$ )	7526 ( $\sim 92\%$ )
Method (C) ( $e=90\%$ )	682 ( $\sim 41\%$ )	1599 ( $\sim 73\%$ )	3612 ( $\sim 973\%$ )	5893 ( $\sim 75\%$ )
Method (C) ( $e=75\%$ )	1238 ( $\sim 74\%$ )	1982 ( $\sim 90\%$ )	1982 ( $\sim 90\%$ )	7100 ( $\sim 90\%$ )
Method (D)	565 ( $\sim 354\%$ )	1978 ( $\sim 90\%$ )	3979 ( $\sim 100\%$ )	6522 ( $\sim 83\%$ )

in AGNs (i.e., Seyfert galaxies and LINERs fainter than  $M_B = -22.25$ ), QSOs (star-like sources with absolute magnitude  $M_B < -22.25$  and broad emission lines) and BL Lacs (confirmed or potential BL Lacs based on optical and radio observations). For the crossmatch, we used a conservative maximum radius of  $1''$  around the position of the radio counterparts for each WIBRaLS, since all coordinates reported in the VERONCAT are based on radio or optical observations and their positional uncertainties are systematically smaller than  $1''$ .<sup>21</sup> We found counterparts in VERONCAT for 797 WIBRaLS ( $\sim 10.1\%$  of the total number of WIBRaLS): based on the classification available in the VERONCAT, 57% of the counterparts are classified as quasars, 13% as Seyferts, 14% as BL Lacs and the remaining  $\sim 16\%$  is classified as generic AGN. It is relevant to emphasize that the classification available in the VERONCAT are not always reliable. For example, a non-negligible fraction of sources classified as BL Lacs in the VERONCAT are not classified as blazars in the ROMA-BZCat (Massaro et al. 2011). In terms of the WISE spectral classification, the cross-matched

WIBRaLS are split in 512 BZQ ( $\sim 52\%$ ) candidates, 213 BZB ( $\sim 20\%$ ) candidate blazars and the remaining 70 WIBRaLS are located in the Mixed region of the *locus* model. The fact that the  $\sim 90\%$  of WIBRaLS cannot be associated to a VERONCAT source likely depends on the lack of optical spectroscopic observations and redshift measurements that are required for a source to be included in the VERONCAT. In particular, given that the optical spectra of BL Lacs are typically featureless and the estimation of the redshift can be problematic, we expect the VERONCAT to miss a large fraction of confirmed blazars. This conclusion is further reinforced by noticing that the positional crossmatch between the most recent version of the ROMA-BZCat and VERONCAT within  $1''$ , only returns 1649 crossmatches on 3149 total sources, corresponding to  $\sim 52.4\%$  of the ROMA-BZCat.

Using the optical B magnitude and radio flux density at 6cm available for a subset of sources in the VERONCAT, we defined as radio-loud AGNs the sources with radio-loudness parameter  $\log R \geq 1$  where  $R = S_{6\text{cm}}/S_B$  is the ratio between the 6cm radio and the B flux densities. We assumed that sources with no radio flux measurement are radio-quiet. We found that 644 out of the 797 total crossmatches ( $\sim 81\%$ ) between the WIBRaLS catalog and VERONCAT obtained with maximum radial distance  $1''$  are radio-loud, suggesting a contamination from radio-quiet AGNs in our catalog smaller than

<sup>21</sup> Using a radius of  $3.3''$ , we found 1618 unique crossmatches with VERONCAT sources. The fractions of different WISE spectral classes of the WIBRaLS associated with this larger radius, and the composition of the crossmatches in terms of the classification available in the VERONCAT are similar to the ones described for the smaller sample obtained with radius  $1''$ .



$\sim 19\%$ . We also checked the contamination from SSRQs in our sample by determining the radio spectral index  $\alpha_R$  between the flux densities measured at 20cm and 6cm, both available for all 644 VERONCAT-WIBRaLS counterparts. We have considered SSRQs the sources with  $\alpha_R > 0.5$ . We found only 73 source which can be classified as SSRQs, corresponding to  $\sim 11\%$  of the total number of VERONCAT counterparts. A more detailed quantitative estimate of the contamination in the WIBRaLS sample introduced by SSRQs is made difficult by the shortage of large catalogs of SSRQs. Nonetheless, based on the result obtained from the VERONCAT, we can assume that the fraction of SSRQs in the WIBRaLS sample will not exceed  $\sim 10\%$ . Furthermore, it has been shown that confirmed BL Lacs from the ROMA-BZCat can have steep radio spectra (see, for instance, Figure 11 in Massaro et al. 2013d), making the observational differences in the definition of the two classes of AGNs less sharp. This fact, in principle, indicates that the effective contamination from SSRQs is smaller than the nominal  $\sim 11\%$  determined here.

We do not observe significant differences between the distributions of the WISE colors and fluxes of the sources that have been associated to a VERONCAT counterparts and the remainder of the WISE blazar-like radio sources. As expected, the WIBRaLS classified as BZB-type candidate blazars are overwhelmingly ( $\sim 92\%$ ) associated with VERONCAT counterparts classified as BL Lac, while the fractions of VERONCAT counterparts classified as BL Lac and associated to WIBRaLS of BZQ-type or Mixed are small ( $\sim 6\%$  and  $\sim 19\%$ , respectively). Even though our results are based on a small subset of the catalog of WIBRaLS crossmatched with a VERONCAT source, they indicate that the fraction of AGNs not classified as blazars is much larger for BZQ and Mixed candidate blazars than for BZB candidate blazars.

## 5. SUMMARY AND CONCLUSIONS

We have presented a catalog of candidate  $\gamma$ -ray blazars extracted from the AllWISE WISE Data Release, using a modified version of the association method for  $\gamma$ -ray unidentified sources from D’Abrusco et al. (2013). This method is based on a model of the three-dimensional *locus* occupied by the confirmed  $\gamma$ -ray emitting blazars in the WISE color space. The WISE blazar-like sources have been spatially associated to radio sources in either the NVSS, FIRST or SUMSS surveys. A further selection based on their radio-loudness has been performed using the  $q_{22}$  parameter to retain only radio-loud AGNs in our sample, and minimize the contamination from other extragalactic radio sources. The main results of this paper can be summarized as follows:

- The final catalog of unique WIBRaLS contains 7855 sources, split in 1682 BZB-type candidate blazars, 3973 BZQ-type candidate blazars and 2194 candidate blazars classified as Mixed. The sky distribution of the members of the catalog reflects the coverage of the radio surveys used and the variable limiting sensitivity of the WISE survey, especially in the [22] filter.
- Out of the total 7855 WIBRaLS, 1295 sources  $\sim 16.5\%$  can be spatially associated to *bona-fide*

blazars in the ROMA-BZCat. The number of WIBRaLS that can be crossmatched with one confirmed  $\gamma$ -ray emitting blazars extracted from the ROMA-BZCat and used to define the model of the *locus* is 454 ( $\sim 76.5\%$  of the *locus* sample). Moreover, 797 WIBRaLS (mostly classified as BZQ according to our method based on WISE colors) can be cross-matched to VERONCAT sources within  $1''$ . Their VERONCAT counterparts are classified as quasars (57%), Seyferts (13%), BL Lacs (14%) and generic AGN ( $\sim 16\%$ ).

- The comparison of the catalog of WIBRaLS with other WISE-based AGN selection techniques suggests that the contamination from non-AGNs in our catalog is very low. While almost all the WISE blazar-like sources classified as BZQ (representing  $\sim 50\%$  of the total sample) are selected by either one of the other techniques, the fraction of WIBRaLS classified as BZB that are recovered by the other methods is significantly lower (from  $\sim 30\%$  to  $\sim 70\%$ ). These difference depends on the fact that BL Lacs candidates (BZB-type WIBRaLS) are significantly bluer than the typical AGNs in WISE, especially in the [3.4] and [4.6] $\mu$ m filters.
- We have estimated the contamination in the WIBRaLS catalog from radio-quiet AGNs and SSRQs. Using a sample of 797 WIBRaLS spatially associated to VERONCAT sources, we found that only  $\sim 19\%$  of our sample can be considered radio-quiet. This fraction represents an upper limit to the contamination because we considered VERONCAT sources missing radio flux density measurements at 6cm radio-quiet. We also confirmed that SSRQs can contaminate the WIBRaLS catalog using a *bona find* sample of 18 SSRQs produced by Gu & Li (2013). Also in this case, using the VERONCAT, we showed that the fraction of SSRQ contaminants in our catalog does not exceed  $\sim 10\%$ .

Our catalog of WISE-selected  $\gamma$ -ray blazar candidates is intended to be a useful resource for the future investigations of the unidentified sources detected in both the  $\gamma$ -ray and X-ray energies. In this paper we do not address the problem of quantifying the effect of several factors that can, in principle, prevent a  $\gamma$ -ray blazar candidate from our catalog to be observed in the current and future  $\gamma$ -ray observations (including variability, intrinsic scatter in the distribution of mid-IR vs  $\gamma$ -ray fluxes for confirmed blazars and the procedure for the source detection in the *Fermi* LAT data). We expect nonetheless that the catalog of WIBRaLS will provide astronomers with a valuable resource to constrain the nature of unidentified high-energy sources.

As an example, Paggi et al. (2013) have shown that a large fraction of the unassociated  $\gamma$ -ray sources located in regions of the sky observed by the X-Ray Telescope (XRT) on board of the *Swift* satellite, can be associated to X-ray counterparts whose coordinates are compatible with the position of WISE candidate blazars selected with the method discussed by D’Abrusco et al. (2013). Moreover, Maselli et al. (2013) have used WISE candidate  $\gamma$ -ray emitting blazars to associate 24 unidentified

hard X-ray sources of the Third Palermo *Swift* Burst Alert Telescope (BAT)<sup>22</sup>. Cowperthwaite et al. (2013) have also used the method for the extraction of candidate  $\gamma$ -ray emitting blazars based on the *locus* in the WISE colors space to associate 13 sources, extracted from the Astronomer’s Telegrams, that exhibit non-periodic variability, mostly at high-energy. These examples clearly show that WISE-based selection of  $\gamma$ -ray emitting candidate blazars can be successfully used to constrain the nature of unidentified high-energy sources observed in different spectral ranges and with different techniques.

The authors thank the anonymous referee for the insightful comments that have helped to significantly improve the manuscript. This investigation is supported by the NASA grants NNX12AO97G and NNX13AP20G. The work by G. Tosti is supported by the ASI/INAF contract I/005/12/0. H. A. Smith acknowledges partial support from NASA/JPL grant RSA 1369566. This research has made use of data obtained from the high-energy Astrophysics Science Archive Research Center (HEASARC) provided by NASA’s Goddard Space Flight Center; the SIMBAD database operated at CDS, Strasbourg, France; the NASA/IPAC Extragalactic Database (NED) operated by the Jet Propulsion Laboratory, California Institute of Technology, under contract with the National Aeronautics and Space Administration. This publication makes use of data products from the Wide-field Infrared Survey Explorer, which is a joint project of the University of California, Los Angeles, and the Jet Propulsion Laboratory/California Institute of Technology, funded by the National Aeronautics and Space Administration. Part of this work is based on the NVSS (NRAO VLA Sky Survey): The National Radio Astronomy Observatory is operated by Associated Universities, Inc., under contract with the National Science Foundation and on the VLA low-frequency Sky Survey (VLSS). The Molonglo Observatory site manager, Duncan Campbell-Wilson, and the staff, Jeff Webb, Michael White and John Barry, are responsible for the smooth operation of Molonglo Observatory Synthesis Telescope (MOST) and the day-to-day observing programme of SUMSS. The WENSS project was a collaboration between the Netherlands Foundation for Research in Astronomy and the Leiden Observatory. We acknowledge the WENSS team consisted of Ger de Bruyn, Yuan Tang, Roeland Rengelink, George Miley, Huub Rottgering, Malcolm Bremer, Martin Bremer, Wim Brouw, Ernst Raimond and David Fullagar for the extensive work aimed at producing the WENSS catalog. TOPCAT<sup>23</sup> (Taylor 2005) for the preparation and manipulation of the tabular data and the images.

## REFERENCES

- Abdo, A. A., Ackermann, M., Agudo, I., et al. 2010, *ApJ*, 716, 30  
 Abdo, A. A., et al. 2014, *ApJS*, in prep.  
 Assef, R. J., Stern, D., Kochanek, C. S., et al. 2013, *ApJ*, 772, 26  
 Becker, R. H., White, R. L., & Helfand, D. J. 1995, *ApJ*, 450, 559  
 Best, P. N., Kauffmann, G., Heckman, T. M., & Ivezić, Ž. 2005, *MNRAS*, 362, 9  
 Bonzini, M., Padovani, P., Mainieri, V., et al. 2013, *MNRAS*, 2553  
 Condon, J. J., Cotton, W. D., Greisen, E. W., et al. 1998, *AJ*, 115, 1693  
 Bonzini, M., Mainieri, V., Padovani, P., et al. 2012, *ApJS*, 203, 15  
 Cowperthwaite, P. S., Massaro, F., D’Abrusco, R., et al. 2013, *AJ*, 146, 110  
 Cutri, R. M., Wright, E. L., Conrow, T., et al. 2011, Explanatory Supplement to the WISE Preliminary Data Release Products, 1  
 D’Abrusco, R., Massaro, F., Ajello, M., et al. 2012, *ApJ*, 748, 68  
 D’Abrusco, R., Massaro, F., Paggi, A., et al. 2013, *ApJS*, 206, 12  
 Donoso, E., Best, P. N., & Kauffmann, G. 2009, *MNRAS*, 392, 617  
 Draine, B. T. 2003, *ARA&A*, 41, 241  
 Gu, M. F., & Li, S.-L. 2013, *A&A*, 554, A51  
 Healey, S. E., Romani, R. W., Taylor, G. B., et al. 2007, *ApJS*, 171, 61  
 Helou, G., Soifer, B. T., & Rowan-Robinson, M. 1985, *ApJ*, 298, L7  
 Jarrett, T. H., Cohen, M., Masci, F., et al. 2011, *ApJ*, 735, 112  
 Kouwenhoven, M. L. A. 2000, *A&AS*, 145, 243  
 Landoni, M. et al. 2014, sub. *A&A*  
 Laurent-Muehleisen, S. A., Kollgaard, R. I., Feigelson, E. D., Brinkmann, W., & Siebert, J. 1999, *ApJ*, 525, 127  
 Masci, F. J. et al. 2001, *PASP*, 113, 10  
 Maselli, A., Massaro, E., Nesci, R., et al. 2010, *A&A*, 512, A74  
 Maselli, A., Massaro, F., Cusumano, G., et al. 2013, *ApJS*, 206, 17  
 Masetti, N., Sbarufatti, B., Parisi, P., et al. 2013, *A&A*, 559, A58  
 Massaro, E., Giommi, P., Leto, C., et al. 2009, *A&A*, 495, 691  
 Massaro, E., Giommi, P., Leto, C., et al. 2011, *Multifrequency Catalogue of Blazars* (3rd Edition), Edited by E. Massaro, P. Giommi, C. Leto, P. Marchegiani, A. Maselli, M. Perri and S. Piranomonte. ARACNE Editrice, Rome, Italy, 118 pages  
 Massaro, F., D’Abrusco, R., Ajello, M., Grindlay, J. E., & Smith, H. A. 2011, *ApJ*, 740, L48  
 Massaro, F., D’Abrusco, R., Giroletti, M., et al. 2013, *ApJS*, 207, 4  
 Massaro, F., D’Abrusco, R., Paggi, A., et al. 2013, *ApJS*, 206, 13  
 Massaro, F., D’Abrusco, R., Paggi, A., et al. 2013, *ApJS*, 209, 10  
 Massaro, F., Giroletti, M., Paggi, A., et al. 2013, *ApJS*, 208, 15  
 Massaro, F., Giroletti, M., D’Abrusco, R. et al. 2014 *ApJS* submitted  
 Massaro, F. et al. 2014, *AJ*, in press  
 Mateos, S., Alonso-Herrero, A., Carrera, F. J., et al. 2012, *MNRAS*, 426, 3271  
 Mateos, S., Alonso-Herrero, A., Carrera, F. J., et al. 2013, *Highlights of Spanish Astrophysics VII*, 288  
 Mauch, T., Murphy, T., Buttery, H. J., et al. 2003, *MNRAS*, 342, 1117  
 Nolan, P. L., Abdo, A. A., Ackermann, M., et al. 2012, *ApJS*, 199, 31  
 Padovani, P., Miller, N., Kellermann, K. I., et al. 2011, *ApJ*, 740, 20  
 Paggi, A., Massaro, F., D’Abrusco, R., et al. 2013, *ApJS*, 209, 9  
 Paggi, A., Milisavljevic, D., Masetti, N. et al. 2014, *AJ*, in pub.  
 Rengelink, R. B., Tang, Y., de Bruyn, A. G., et al. 1997, *A&AS*, 124, 259  
 Sargent, M. T., Schinnerer, E., Murphy, E., et al. 2010, *ApJS*, 186, 341  
 Shaw, M. S., Romani, R. W., Cotter, G., et al. 2013, *ApJ*, 764, 135  
 Stern, D., Eisenhardt, P., Gorjian, V., et al. 2005, *ApJ*, 631, 163  
 Stern, D., Assef, R. J., Benford, D. J., et al. 2012, *ApJ*, 753, 30  
 Stickel, M., Padovani, P., Urry, C. M., Fried, J. W., & Kuehr, H. 1991, *ApJ*, 374, 431  
 Stocke, Jc. T., Morris, S. L., Gioia, I. M., et al. 1991, *ApJS*, 76, 813  
 Sutherland, W. & Saunders, W. 1992 *MNRAS*, 259, 413  
 Taylor, M. B. 2005, *Astronomical Data Analysis Software and Systems XIV*, 347, 29  
 Urry, C. M., & Padovani, P. 1995, *PASP*, 107, 803  
 Véron-Cetty, M.-P., & Véron, P. 2010, *A&A*, 518, A10  
 White, R. L., Becker, R. H., Helfand, D. J., & Gregg, M. D. 1997, *ApJ*, 475, 479  
 Wright, E. L., Eisenhardt, P. R. M., Mainzer, A. K., et al. 2010, *AJ*, 140, 1868

<sup>22</sup> <http://www.ifc.inaf.it/cgi-bin/INAF/pub.cgi?href=activities/bat/index.html>

<sup>23</sup> <http://www.star.bris.ac.uk/~mbt/topcat/>